TERRA LATINOAMERICANA



Model of Water Flow Infiltration Force in a Soil Mass Modelo de Fuerza de Infiltración de Flujo de Agua en una Masa de Suelo

Eduardo Teófilo-Salvador^{1‡}

- ¹ Universidad Nacional Autónoma de México, Facultad de Ingeniería, División de Ingeniería en Ciencias de la Tierra. Circuito Escolar s/n, Ciudad Universitaria. 04510 Coyoacán Ciudad de México, México; (E.T.S.).
- [‡] Corresponding author: teofilo.salvador@ciencias.unam.mx

SUMMARY

The flow of water in the soil generates processes that can be passive and active and manifest themselves in different ways. The objective was to propose a mathematical model to estimate the infiltration force of water in the soil in three components. It was based on formulations of Hydrology, Newton's Law, and hydrogeology, and the water flow-soil mass system was identified through vertical, lateral, and superficial infiltration. To apply the formulations, reported data and experimental review of a multifunctional infiltrometer were used, and dry, saturated, and supersaturated soil masses were chosen. It has been obtained that the proposed model relates the variation of the infiltration force in direction, magnitude, and distribution, even for the same type of soil, the displacement is at different instantaneous speeds, due to the moisture content, porosity, hydraulic conductivity, and depth of the soil profile. The limitation is that no more multifunctional infiltrometers have been developed to apply the proposed model, but the results obtained can be associated with: i) if the vertical infiltration force predominates, there is greater effective infiltration as the first impulse of recharge, ii) if the lateral force predominates, the presence of soil instabilities, such as landslides, is possible, and iii) if the surface force predominates, the result is runoff or flooding on the soil.

Index words: infiltration-effective, instability-soil, runoff-flood.

RESUMEN

El flujo de agua en el suelo genera procesos que pueden ser pasivos y activos y se manifiestan de formas diversas. El objetivo fue proponer un modelo matemático para estimar la fuerza de infiltración de aqua en el suelo en tres componentes. Se partió de formulaciones de hidrología, la Ley de Newton e hidrogeología, se identificó el sistema flujo de agua - masa de suelo mediante infiltración vertical, lateral y superficial. Para aplicar las formulaciones, se utilizaron datos reportados y de revisión experimental de un infiltrómetro multifuncional, se eligieron masas de suelo secas, saturadas y sobresaturadas. Se ha obtenido que el modelo propuesto relaciona la variación de la fuerza de infiltración en dirección, magnitud y distribución, incluso para la misma clase de suelo el desplazamiento es a diferentes velocidades instantáneas, debido al contenido de humedad, porosidad, conductividad hidráulica y profundidad del perfil del suelo. La limitante es que no se han desarrollado más infiltrómetros multifuncionales para aplicar el modelo planteado, pero los resultados obtenidos pueden asociarse a: i) si la fuerza de infiltración vertical predomina hay mayor infiltración eficaz como primer impulso de recarga, ii) si predomina la fuerza lateral es posible la presencia de inestabilidades de suelo, como deslizamientos, y iii) si predomina la fuerza superficial el resultado es escurrimiento o inundación sobre el suelo.

Palabras clave: infiltración-eficaz, inestabilidad-suelo, escurrimiento-inundación.



Recommended citation:

Teófilo-Salvador, E. (2025). Model of Water Flow Infiltration Force in a Soil Mass. *Terra Latinoamericana*, 43, 1-13. e2186. https://doi.org/10.28940/terra. v43i.2186

Received: December 3, 2024. Accepted: May 20, 2025. Article, Volume 43. October 2025.

Section Editor: Dr. Antonio Juárez-Maldonado

Technical Editor: M. C. Ayenia Carolina Rosales Nieblas



Copyright: © 2025 by the authors. Submitted for possible open access publication under the terms and conditions of the Creative Commons Attribution (CC BY NC ND) License (https://creativecommons.org/licenses/by-nc-nd/4.0/).

INTRODUCTION

The water-soil process is complex when they are associated with hydrometeorological phenomena (Gascón et al., 2013). The flow of water in unsaturated soils depends on internal factors as hydraulic gradient and retention, for which constitutive relations that describe fluid flow, strength, and deformation behavior of variably saturated soils are the soil-water retention curve, hydraulic conductivity function, and suction-stress characteristic curve, are valid for a tested range (Lu, Kaya, and Godt, 2014). But, external factors as the intensity, duration, and distribution trajectories of rainfall also influence (Díaz-Puga and Mateos, 2013). In addition, the infiltration rate and vertical displacement for different rainfall intensities and durations can be nonlinear in the soils (Chatra, Dodagoudar, and Maji, 2017).

According to Estabragh, Soltani, and Javadi (2016), as the water flows through the soil, a force is applied to the soil particles, which is referred to as infiltration force, and forces exist whenever there is a gradient of head in a permeable unit that allows water movement (Tomlinson and Vaid, 2000). The infiltration and vertical pressure eventually result in lateral pulses due to the water pressure that can generate mass landslides and differential displacements (Priest et al., 2011). The vertical and lateral hydraulic conductivity are different; in addition to that, the lateral flow occurs in inclined interfaces during a stationary percolation (Miyazaki, 1988). Thus, hydraulic behavior strongly influences the manifestation of deformations (Garcia, Oka, and Kimoto, 2011).

Vertical flow is associated with groundwater recharge and lateral flow as a component in dynamic processes that control the subsurface flow mechanism (Teófilo-Salvador, Morales, Esteller, and Muciño, 2019a). The process of spatial distribution of water in the soil can be as subsurface flow in the soil matrix or through macropores and surface runoff, which play an important role in sloping land (Van Asch, Van Dijck, and Hendriks, 2001), where the main force of the superficial flow is due to the inclination (Tosaka, Itoh, and Furuno, 2000), with which the speed is greater and the depth of advance inside the ground becomes superficial, thus, the horizontal velocity depends on the hydraulic conductivity of the soil (Hsieh and Yang, 2011). But if the soil is coarse-grained and high infiltration rates are generated, positive pressure develops, and the infiltration force causes instability of the soil within the slope (Collins and Znidarcic, 2004). The flow vectors within the soil mass converge towards points where there is exit to the exterior (Kosugi, Uchida, and Mizuyama, 2004), such as macropores by microfauna or rooting, where eventually the highest peak of the reinforcement can be found from 0.1 to 0.2 m of depth, which varies laterally and vertically as well as decaying with increasing depth (Montgomery, Schmidt, Dietrich, and McKean, 2009).

Currently, the models provide insufficient information about the subsurface flow induced by rain and the effect of lateral flow along the soil interface, such that a physical or mechanical and infiltration coupling is necessary that incorporates a change technique to address flow and soil problems (Huang and Lo, 2013). The effect of the flow infiltration forces is very important, since they vary spatially. However, some authors indicate that the magnitude and direction of these forces are independent variables. Still, it is not clear how the spatial distribution of these forces is introduced (Li, Rendón, and Espinoza, 2010). Besides that, according to Zhong, Hao, and Xi (2018), it is necessary to consider the hydraulic conductivity to calculate and reflect the stability of soils in response to changes such as the gradual expansion with an increase in the amount of rainfall.

However, less research has focused on the various intensive seepage degrees and locations on fluid spills in soils (Huang, Bai, and Xu, 2022); also the soil particle movement under seepage flow is one of the predominant mechanisms responsible for incidents and failures, or the reduction of the stress of the particles generating erosion by increasing the filtration force (Ghafoori, 2024; Ghafoori, Maček, Vidmar, Říha, and Kryžanowski, 2020; Xiao and Wang, 2020; Huang, Bai, Xu, Cao, and Hu, 2017). Seepage induced instabilities pose a challenge in many geotechnical, engineering, geology applications, and current understanding is based on a global perspective that draws on continuum mechanics, in lab tests, experimental tests, and numerical simulations (Sanvitale, Zhao, Bowman, and O'Sullivan, 2023). Another effect is the runoff generated by rainfall flow. This surface runoff is important if antecedent soil moisture is high, or if the maximum infiltration rate at the surface is lower than the actual rainfall intensity (Bronstert, Niehoff, and Schiffler, 2023). Excessive surface saturation leads to eventual flooding. In this context, current surface-subsurface flow models still present challenges such as: i) the actual rainfall intensity may vary over time; ii) the infiltrability of the soil surface may be reduced, due to crusting, compaction or sealing of the soil surface, or hydrophobic effects; iii) or soil infiltration may increase as a consequence of preferential flow paths or macropores such as bioturbations or other voids. Thus, water infiltration into soil contributes to environmental benefits and damages of global interest, but little has been characterized in a quantitative and refined way, as a soil-water interaction (Han, Wang, Liu, and Li, 2022), of particular interest in the practice of engineering, hydrogeology, hydraulics, and geomechanics. Based on the above, the objective of the research was to propose a model to determine the infiltration force of water in the soil from the conceptualization of the components of flow and its revision with experimental tests.

MATERIALS AND METHODS

Conceptualization of the Water Infiltration Process in the Soil

The water from rainfall, irrigation or flood, in soils can be distributed of the form: i) P = I + RO; P is the rainfall and controls the saturation of the soil, RO runoff and I infiltration. ii) $I = \Delta\theta + DP$; in excess of water in the soil, the evapotranspiration of the crop can be disregarded (Teófilo-Salvador et al., 2019a), only the moisture content of water in the soil $\Delta\theta$ is related, and with it the deep percolation (DP). iii) $DP = IE + \Delta FS$; the topographic influence on the distribution of the flow throughout the thickness of the root zone promotes the initial effective infiltration (IE) towards the unsaturated zone and subsurface flow (ΔFS) in the lateral direction. iv) $P = RO + \Delta\theta + IE + \Delta FS$; when the underlying soil layer has low hydraulic conductivity, the vertical flow is reduced, thereby reducing the initial effective infiltration, and the presence of frequent, intense, and prolonged rains increases the lateral flow, moving above this underlying layer (Teófilo-Salvador, Morales, Muciño, and Esteller, 2019b).

Assuming that: 1) there is a source of water flow supply to the ground, 2) the superficial flow begins which is preceded by the lateral flow and in turn this is preceded by the vertical, 3) with the saturated soil the surface runoff begins and with it a supersaturation, giving rise to a lateral drainage which will contribute to a subsuperficial flow (Figure 1). The subsurface flow depends directly on any source (rain, reservoir, open channels, pipes, e.g.) near or on the surface and can be moved at the same rate as the incidence of what originates it, or so slow that it allows you to move vertically and laterally. But if the porous medium does not allow a rapid transit, then there will be a superficial flow, also if there are plant barriers or obstacles, these can modify the movement and can generate the runoff-filtration process.

Therefore, they set out infiltration trajectories; a vertical, lateral and superficial infiltration, with a geometric pattern due of the hydraulic gradient for each component. That is, as the depth of advance z increases, the area perpendicular to the flow increases in time and, therefore, the volume of influence of each component. Whereas, on the surface, the forces tend downwards with a maximum hydraulic gradient, and as the depth increases, the infiltration vectors turn towards the face of the slope, although apparent mass movement is possible, such as a partially confined flow parallel to the main axes (Lima and Correa, 2018).

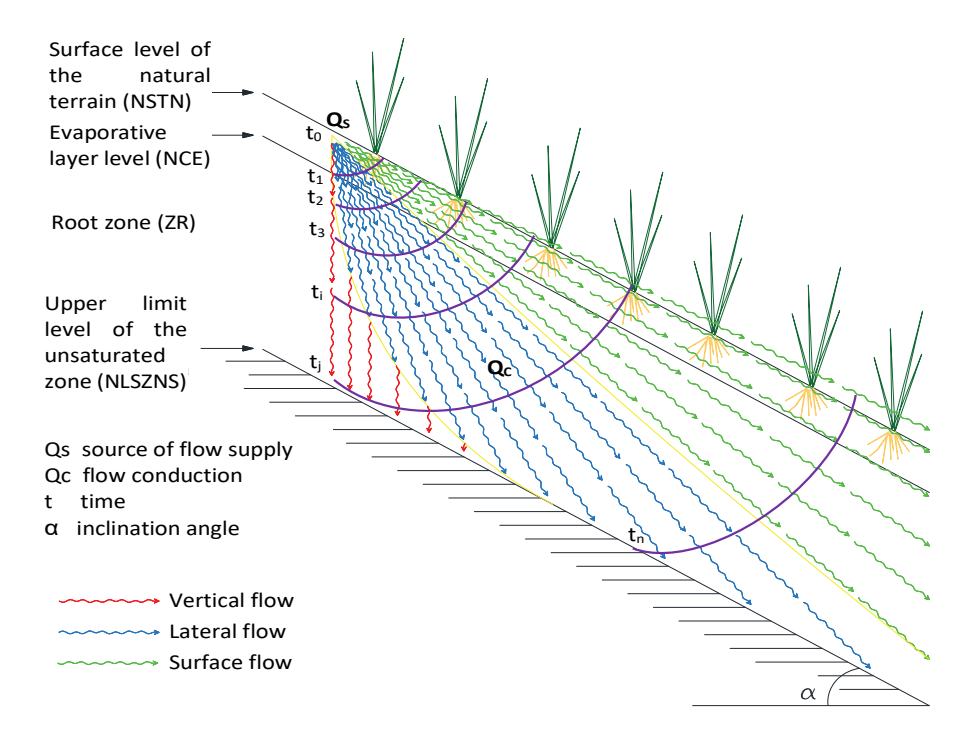


Figure 1. Conceptual model of movement of water flow in the soil (Own elaboration).

Preliminary Relations

When the soil is not saturated, there is an average rate of water distribution in the pores $V_{dp'}$ with the flow of Darcy q and the volumetric content of water θ (Miyazaki, 2006), equation (1):

$$V_{dp} = \frac{q}{\theta} \tag{1}$$

If the soil is continuously wet the variation moisture content are small, with constant tendency, then the hydraulic load is negligible compared to other forces (gravity or inertia), in such a way that the flow is equivalent to the hydraulic conductivity, equation (2):

$$V_{dp} = -\frac{k}{\theta} \tag{2}$$

In this way, the fluid moves at an average infiltration rate (V_s) within the soil mass associated with the porosity (n), so the equation (3):

$$V_s = \frac{q}{n} \tag{3}$$

Once the soil is saturated, the distribution of water in the pores increases and decreases at an almost trickle discharge rate, which is the most representative pulse (Elmaloglou and Diamantopoulos, 2008), so a supersaturation of the ground forces the start of a download rate (V_d), shown as equation (4)

$$V_d = ki \tag{4}$$

Where i is the hydraulic gradient, in addition to considering continuous flow and the effect of porosity, it is possible to combine equations (3) and (4), leaving equation (5):

$$V_s = \frac{V_d}{n} \tag{5}$$

These expressions can be applied to saturated, partially saturated, or unsaturated soil, with the difference that in the first case the hydraulic conductivity is constant, and in the second case it varies depending on the moisture content (López-Acosta, 2014). The hydraulic gradient is a vector that describes the slope of the energy distributed within the soil (Radcliffe and Rasmussen, 2002), so the terms were reordered to leave them in terms of *i*, resulting in the equation (6):

$$i = \frac{V_s n}{k} \tag{6}$$

Infiltration force

Starting from Newton's second Law, where the force is the equation (7):

$$F = mg (7)$$

In the case of the flow of water on sloping ground, it generates an infiltration force that involves the hydraulic gradient i, the density is constant ρ_w and the volume of influence is equal to the depth of advance dz by the differential area perpendicular or normal to the direction of transfer of the water flow, such that it can be expressed as the equation (8):

$$F = \rho_{w} i dz \cdot dx dy \tag{8}$$

Regrouping the terms of Eq. (6) in Eq. (8), you get to the water infiltration force equation in the soil, equation (9):

$$F = \rho_{w} n \frac{V_{s}}{k} (dz) \cdot (dy dx) \tag{9}$$

Where if the change in moisture content is large (not saturated - saturated - oversaturated), the average infiltration rate is expressed as a of change with respect to time for a certain hydraulic load (dh/dt), then it is assumed that from the source of supply rain or hydraulic load on the surface. Any variation in the internal filtration rate can be identified at carry out the measurement by means of hydraulic loads on the surface as a function of the measurement time, when dh/dt is constant in a steady state (Rausch, 2009), that is, the charge decreases equally with time, but in a transient state dh/dt varies as it happens in an infiltration curve measured in the field, it can be estimated as the volume of water that flows from one point to another over some time is estimated by measuring time dependent changes in the water content profile, similarly the hydraulic gradient (Lu and Likos, 2004), leaving the equation (10):

$$F = \rho_{w} \frac{n}{k} \left(\frac{dh}{dt} \right) (dz) \cdot (dydx) \tag{10}$$

Equation 10 shows; i) dh/kdt is the behavior of the water flow in time as it is conducted in the soil mass, that is, the rate of distribution is a function of depth, in this way the hydraulic conductivity can be evaluates with the concentric cylinder infiltrometer (Neris, Jiménez, Fuentes, Morillas, and Tejedor, 2012), ii) the porosity n that is a property of the soil mass, and iii) the property of the liquid ρ_w . Thus, the volumetric measure of the advance of the water flow in the soil is obtained with dzdydx.

The relationship between equations 3 and 10 is that the first evaluates the average infiltration rate within the soil mass, and equation 10 includes the rate through the variation of the hydraulic head over time, on volumetric and property effects of the fluid, such that dh/dt can be evaluated with the concentric cylinder infiltrometer. Considering three trajectories defined as infiltration force vectors, a vertical, a lateral, and a superficial (Figure 2), whose distribution range depends on the incidence of water in the soil, the initial moisture content, texture, cover vegetation, land use, and land slope.

The angle of the vertical infiltration force is 90°, the angle of the lateral infiltration force is β_1 , and the angle of the surface infiltration force is β_2 ; thus, any angle formed between the three vectors is less than 45°, within the allowable values between 0 and 45° (Budhu and Gobin, 1996).

 $F_{v'}$, and F_{s} are the vertical, lateral, and surface forces of equation (11a-c), deduced in this investigation.

$$F_{V} = \rho_{w} \frac{n}{k_{v}} \left(\frac{dh_{v}}{dt} \right) \left(\int_{z=0}^{z=\frac{Z}{\cos \alpha}} dz \right) \left(\int_{y=0}^{y=y_{1}} dy \right) \left(\int_{x=0}^{x=x_{1}} dx \right)$$
 (11a)

$$F_{L} = \rho_{w} \frac{n}{k_{l}} \left(\frac{dh_{l}}{dt} \right) \left[\int_{z=0}^{z=\frac{Z}{\cos \alpha}} \frac{dz}{dx} \right] \left(\int_{y=0}^{y=y_{1}} dy \right) \left(sen(90 - \beta_{1}) \int_{x=0}^{x=x_{1}} dx \right)$$

$$(11b)$$

$$F_{S} = \rho_{w} \frac{n}{k_{s}} \left(\frac{dh_{s}}{dt}\right) \left[\int_{z=0}^{z=\frac{Z}{\cos\alpha}} dz \int_{y=0}^{y=y_{1}} dy \right] \left(sen\alpha \right) \int_{x=0}^{x=x_{1}} dx$$
(11c)

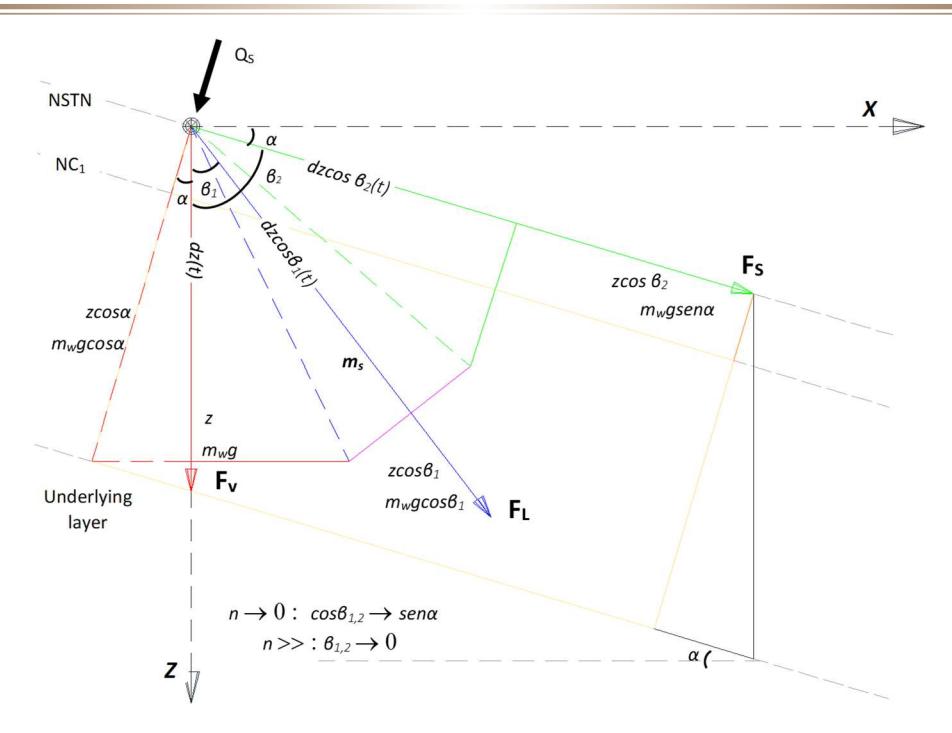


Figure 2. Conceptual model of water infiltration force in the soil (Own elaboration).

Where dh/dt and dh/dt and dh/dt are the average infiltration rates (f) vertical, lateral and superficial, since according to Griffiths and Lu (2005), the instability does not only depend on the water and type of soil, too of the infiltration rate. The k_v and k_l are the vertical and lateral effective saturated hydraulics conductivities respectively, and a surface effective saturated hydraulic conductivity k_s . The sum of the three infiltration forces is equal to the resultant force generated by the subsurface flow ΔFS , a relationship such as the equation (12):

$$\Delta E \rightarrow F_{\Lambda E} = F_V + F_I + F_S \tag{12}$$

The units of the force remain in unit of mass [M]. So, simplifying equations (11a), (11b) and (11c), we get to equation (13a), (13b) and (13c):

$$F_V = \rho_w n \frac{f_v}{k_v} z A_v \tag{13a}$$

$$F_{L} = \rho_{w} n \frac{f_{l}}{k_{l}} \left[\frac{z}{\cos(\beta_{1})} \right] A_{l}$$
 (13b)

$$F_{s} = \rho_{w} n \frac{f_{s}}{k_{s}} \left[\frac{z}{\cos(\beta_{2})} \right] A_{s}$$
 (13c)

These deduced expressions being those that make up the proposed filtration force model in this research. And this developed due to the changes in the yield stresses caused by infiltration force, which are generated by fluid pressure gradients (Rozhko, 2010).

Initial and Boundary Conditions

The system is valid for homogeneous and isotropic medium, where, thus the evaluation limits of the infiltration force in the first layer of soil are the equation (14):

$$F_{V,L,S}: f(x,y,z,t)\Big|_{z=0}^{z=\frac{Z}{\cos\alpha}}\Big|_{t=0}^{t=t_n}$$
(14)

So, the boundary conditions for the proposed system are the equation (15):

$$F(z=0,t) = F_0$$

$$F(z=\frac{Z}{\cos\alpha},t) = F_1$$
(15)

And the initial condition is the equation (16):

$$F(z,t=0) = 0 \tag{16}$$

Thus, with the above it is possible to estimate in the equation (17):

$$z = 0 \quad a \quad z = \frac{Z}{\cos \alpha}$$

$$t = 0 \quad a \quad t = t_n$$

$$F_R = F(z, t)$$
(17)

Where FR is the resulting infiltration force vector.

Application of the Model with Experimental Measurements

It was necessary to perform in situ experiments to measure the infiltration rate, for which the redesigned multifunctional concentric cylinder infiltrometer was used (Teófilo-Salvador et al., 2019b; Teófilo-Salvador and Morales-Reyes, 2018), especially for different moisture contents of the soil from dry to saturated. Since obtaining real results, it is preferable to saturate the border in a certain time and avoid imposing hydraulic loads on the surface (Lazarovitch, Ben, Šimůnek, and Shani, 2007). So, the team reproduced a combination of certain rainfall intensities, since according to Chhorn, Hong, and Lee (2014) it is not so relevant to choose high values to generate soil instability, besides that also the inclination angle had to be spatially varied (Li et al., 2010).

Likewise, soil parameters were determined in the soil mechanics laboratory based on Teófilo-Salvador et al. (2019a), Teófilo-Salvador et al. (2019b), Teófilo-Salvador, Morales, Muciño, and Esteller (2019c) y Teófilo-Salvador y Morales (2018). To ensure that the number and spacing of soil samples in the field were representative of the root zone and the LSZNS, stratified random sampling was followed (Walpole, Myers, Myers, and Ye, 2012). A telescopic borer was used to extract the soil samples; the depth of each hole was measured, and a quantity of water was poured into it to quantify the volume. This was used to determine the volumetric weight (Coras, 1989). The samples were weighed in the laboratory; some were dried in an electric oven at 110 °C, and others were left outdoors to prevent the disintegration of organic matter. The moisture content, density, porosity, and equivalent water layer were obtained from the samples. Samples were divided into 600 to 1000 g samples for sieving, grain size percentages were weighed, and the textural class was determined (USDA, 2004). The field data were analyzed as follows: when the hydraulic head was kept constant to avoid null values when using the infiltrometer, a distribution over time was made, both for readings of the inner, intermediate and outer cylinders. The duration of the test record was 1.06 h to 4.41 h, with average rainfall intensities of 22 mm h⁻¹ to 384 mm h^{-1} (Teófilo-Salvador et al., 2019b). Subsequently, the Kostiakov model was applied to generate the adjustment of each curve of the infiltration rate, accumulated infiltration and from this to evaluate the basic and saturated conductivity in the test period. Consecutively, the filtration force was determined, for which formulations (10) and (11) were applied, where the depth of advance z was varied as a function of k, and the area with x and y, since the hydraulic conductivity varied according to the time of tests, according to Kostiakov's adjustments, with respect to the angle of inclination, it was left parallel to the z axis for the vertical force, for the lateral it was assumed from 270 $^\circ$ to 290° (angle measured counterclockwise) according to what was observed in the field, and the superficial one of 310°, and the resulting force as a contribution of each of the forces obtained, for an angle of ground inclination of 35°, these calculations were programmed in Microsoft Excel®.

Additionally, it was corroborated by linking the calculation sheets from the field data and soil sampling, for the root zone: sandy-loam and sandy-clay-loam type, natural density of 0.77 g cm⁻³ to 1.40 g cm⁻³, moisture content of 7.43% to 20.68%, porosity of 9.0% to 19.30% and equivalent water layer of 33.57 mm to 102.19 mm. For the underlying layer: sandy type, natural density of 1.91 g cm⁻³ to 2.21 g cm⁻³, moisture content of 18.14% to 53.75%, porosity of 17.08% to 38.95% and equivalent water layer of 19.81 mm to 34.96 mm (Teófilo-Salvador *et al.*, 2019b). With the adjustment of the infiltration rate and hydraulic conductivity, and finally with the filtration force, that is, applying the simplified equations (13). And the procedure was repetitive for each test under different humidity conditions. Equivalent water layer of the soil previous from 49.09 mm to 46.80 mm, subsequent from 139.48 mm to 158.18 mm, and retained from 90.39 mm to 142.69 milimeters.

RESULTS AND DISCUSSION

Applying the model in dry soil (Figure 3), the surface flow rate in dry soil is constant, the accumulated infiltration force tends to be curved decreasing instantaneously, for the case of vertical force this presents a linear behavior with depth of advance similar to that of the surface component, and the difference between vertical and lateral force is attributed to free flow above the layer underlying the root zone. Essentially, vertical filtration is appreciated, since when the soil is dry, the flux tends to move primarily in the z axis, as observed in the field, there was no presence of noticeable surface flow. During 1.2 h of testing, the advancement depth was 140 mm, 190 mm, and 160 mm, vertical, lateral, and superficial, respectively. For a unit area, the resulting filtration force as the sum of the three components was close to 700 kg, at an average infiltration rate of 50 mm h⁻¹. But this load is distributed over the test time, such that as the infiltration rate decreases or increases, expansion/tension cracks or pipes can form in the soil, so the effect of the accumulated force is released into the atmosphere. The surface force decays more rapidly at 0.75 h, the vertical force reaches 20 kg at 0.86 h, but the lateral force persists, being the predominant one at longer times and depths.

Figure 4 shows that, for a soil with a history of humidity to a saturated degree, the behavior of infiltration force is more extended to the right compared to the dry case, which generated a more curved pattern for the three components. In this case, the lateral infiltration force was greater than the superficial and vertical, even with lower infiltration rates compared to the dry case. Thus, it can also be observed that the vertical component of flow depends on the infiltration rate, which is decreasing, so in saturated soil, it can be negligible; that is, the

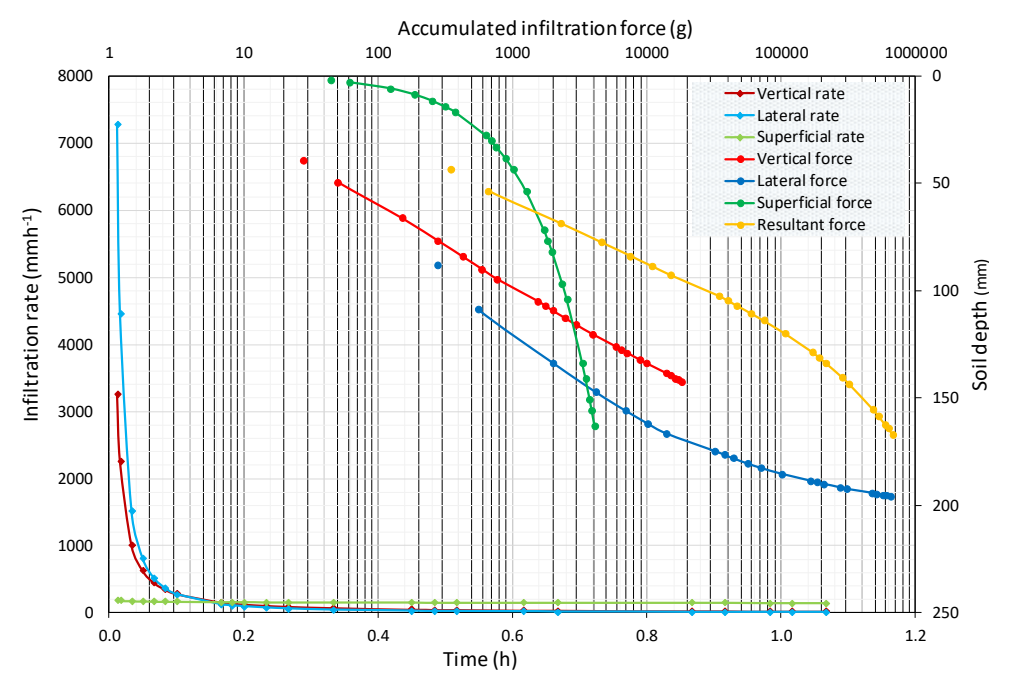


Figure 3. Infiltration force for a dry soil (Own elaboration based on data of Teófilo-Salvador et al., 2019b; 2019c).

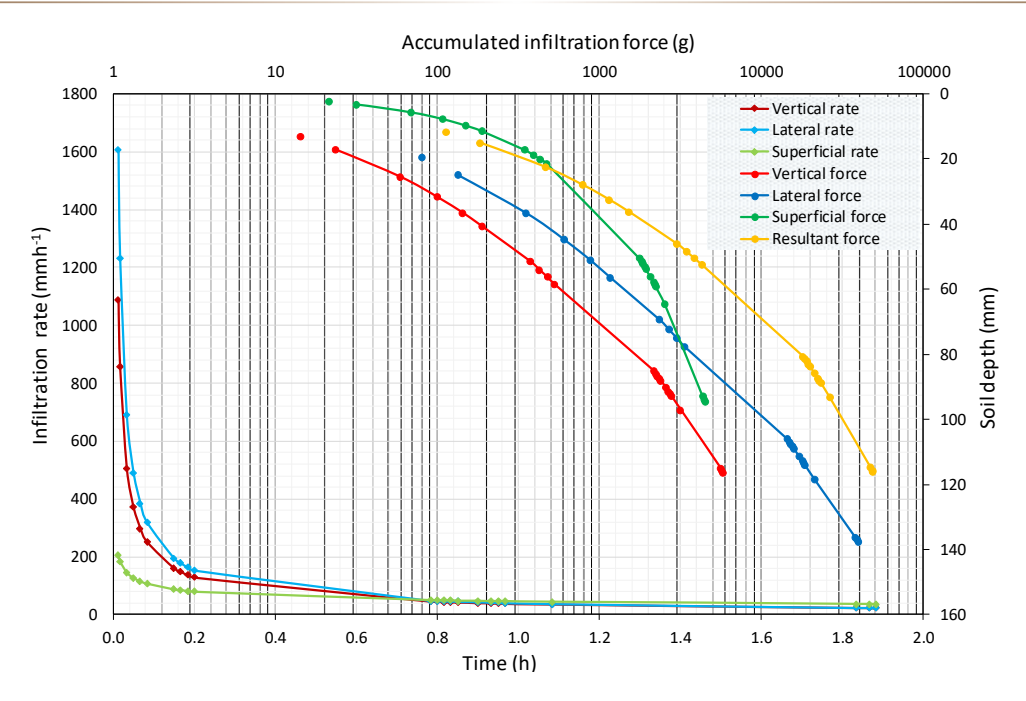


Figure 4. Infiltration force for a saturated soil (Own elaboration based on data of Teófilo-Salvador et al., 2019b; 2019c).

flow length is much greater than the infiltrated sheet. Therefore, the infiltration force in the soil mass depends on meteorological (rainfall), hydrogeological (hydraulic conductivity), edaphological (porosity), mechanical (stress-strain-displacement), and physical (water flow in the soil mass) characteristics; besides that, said flow increases the weight of the soil. During 1.9 h of testing, the advancement depth was 116 mm, 138 mm, and 94 mm, vertical, lateral, and superficial, respectively. For a unit area, the resulting filtration force as the sum of the three components was 50 kg, at an average infiltration rate of 40 mm h⁻¹. At 1.45 h the surface force stabilizes at 9.5 cm depth, the vertical force stabilizes at 1.5 h at a depth of 12 cm, and the lateral force at a time greater than 1.8 h with a depth of 14 cm. Thus, water that cannot seep through the soil pores creates a backlog of flow, which reduces soil permeability and thus decreases the infiltration rate (Zulkarnain, Kurniawati, Triwulandari, Husein, and Kurniawan, 2023).

In the case of supersaturated soil, the vertical component has a lower magnitude, and the lateral force mainly influences the superficial one, attributed to the internal pressure of the flow by the hydraulic load (Figure 5). The behavior of the infiltration force is independent of the infiltration rate, due to the porosity and hydraulic conductivity of the soil, which have greater weight on other variables such as the depth of advance. Additionally, the resulting forces show a weighting of the force vector magnitude, but it does not allow for defining which component is of greater importance, for example, for the study of soil instabilities associated with stress, deformations, and displacement. Finally, for 1.3 h of testing, the advancement depths of 175 mm, 320 mm, and 220 mm were obtained, vertical, lateral, and superficial, respectively. For a unit area, the resulting filtration force as the sum of the three components was 50 kg, at an average infiltration rate of 85 mm h⁻¹ and 180 mm h⁻¹. Near 1 h the vertical force tends to stabilize at 0.17 cm, and the surface force up to 1.1 h at 0.21 cm, with the lateral force being of greater relevance for the test time period at a depth of greater than 0.30 centimeters.

The high values of the infiltration rate are attributed to the tubifications observed in the field, which generate preferential flows. Due to the heterogeneity of the soil in samples and experiments, possible desiccation cracks can induce preferential flow in cracked soils, causing rapid infiltration of water into shallow soils, so rainfall-evaporation cycles are also important (Luo et al., 2021), in addition to surface-subsurface processes.

In this way, it is verified that evidently the superficial component of flow generates the minimum stability. The infiltration force represents a force proportional to the potential of the hydraulic gradient, which may be responsible for the instability of soil, in such a way that physically the infiltration force can have greater influence than the high pore pressures, since according to Feng, Liu, and Ng (2019) this is reduced by the effect of vegetation through the absorption of water from the root (uniform, triangular, exponential or parabolic).

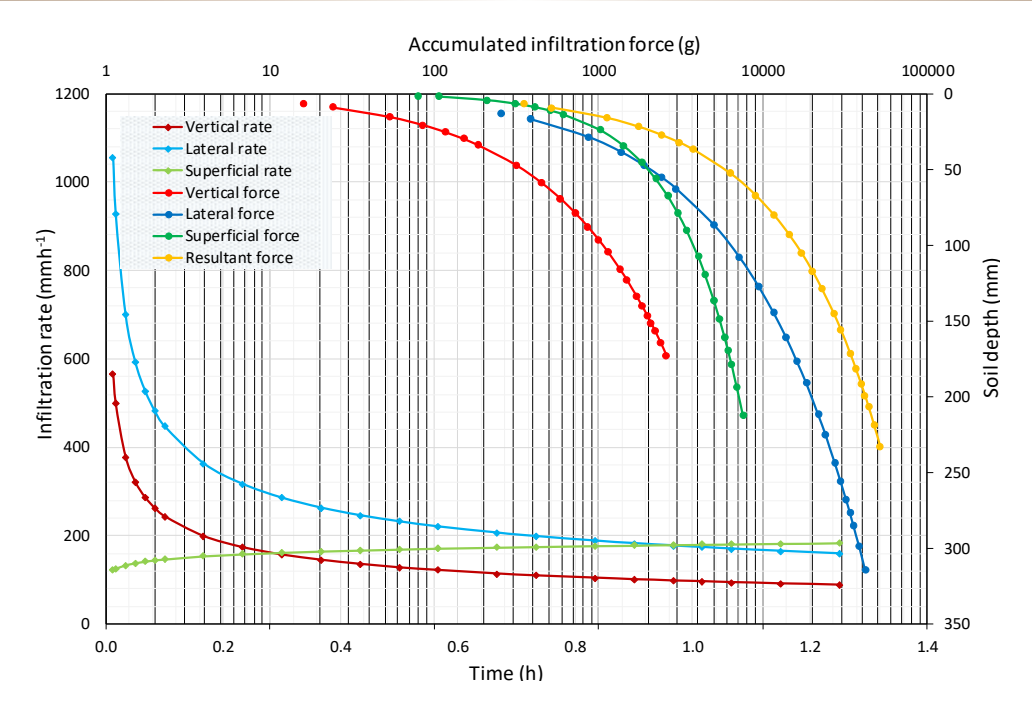


Figure 5. Infiltration force for an oversaturated soil (Own elaboration based on data of Teófilo-Salvador et al., 2019b; 2019c).

The results are sensitive to the initial conditions; for example, vertical infiltration depends on soil moisture. When the saturated permeability of the soil was greater than the rainfall intensity, the flow was essentially vertical; otherwise, the movement of the water was lateral. When the hydraulic gradient was high, it gave a pattern to erosion and/or tubing. Therefore, in well-drained soil, the flow vectors converged around the tubing generated by the macropores; for that reason, the pore pressure was disregarded, but as there were no connected macropores with an exit to the atmosphere, the infiltration force increased, generating mobilization of the soil mass.

For soil with high compaction, the rate of water infiltration was reduced, agreeing with Udawatta, Gantzer, Anderson, and Assouline (2016); for that reason, it was reflected in the advance of the flow in the vertical and later lateral directions. Like Huang, Lee, Ho, Chiu, and Cheng (2012), but for this investigation it was found that the nature of rainfall patterns are not the main factor that controlled the stability of the soil, but the force exerted by the water within the porous medium, such that if the density of the soil tends to zero the vectors of vertical, lateral and superficial force converge toward the z axis, thus water flows at a higher rate compared to an increase in density value, where the vertical vector decreases and increases the surface vector leading to the erosion process.

In this way, the proposed model incorporates a realistic effect, compared to the formulations used by Bierawski and Maeno (2006) for calculating the vertical and lateral force components. In addition, the main contribution of this research is that the infiltration forces can cause a significant threat to the stability of soils, while the effective pressure can be distributed in the medium (Shin, Song, Lee, and Cho, 2011). Also, a change in soil density from permeable to a more impermeable one generates changes in the process regardless of the depth of the stratum, such that the perpendicular area changes as the water flow progresses, as does the average infiltration rate.

It is convenient to apply the technique in other places, considering a simplified coupling with the vegetation, since the conditions of the soil surface, the state of humidity, and vegetation play important roles in these processes (Xiang, Vivoni, and Gochis, 2018). In addition, the infiltration rate changes depending on the composition and texture of the soil. Since the infiltration force arising from the water flow is one of many important factors contributing to slope failure (Pan, Xu, and Dias, 2017).

CONCLUSIONS

The infiltration of the water flow in the soil generates some force, which was described from Newton's second Law, where the porosity of the soil is related, the density of the water flow in a geometric medium. The infiltration pressure can be described in terms of the infiltration force, which can lead to a displacement of the flow and a displacement of the soil. The combination of these two displacements allows for estimating a compound displacement if the soil undergoes dynamic changes due to meteorological and mechanical or physical conditions of the porous medium. With this model, it is verified that the infiltration force varies in direction, magnitude, and distribution.

According to the model, i) when the vertical seepage force predominates, it is assumed that there is purely recharge of the water to deeper layers, ii) when the lateral force predominates, the presence of differential movements and displacements is possible due to the increase in mass and the effect of the slope of the soil with possible cracks of tension, and iii) when governing surface seepage, runoff will predominate due to saturation in underlying layers, topographic changes or material with a high degree of compaction, causing eventual flooding. In this way, the porosity can change during or after the filtration process, such as the contraction-expansion of the soil, as a hysteresis process.

The trajectories of the water flow in soils change due to the gravity and force of the pressure gradient, by such they move to different instantaneous rates, and the behavior varies in function of the content of humidity, of the porosity of the layers involved, the hydraulic conductivity and the depth, as observed in the field and when analyzing the data with the model.

To apply the model proposed in this research, field sampling and laboratory treatment are required, as well as experimental measurements of the three infiltration components: vertical, lateral, and surface, determined using a redesigned multifunctional concentric cylinder infiltrometer or another device that allows estimating the three variables. The main innovation of this research is the coupling of experimental, field, laboratory, and theoretical variables into the processes that trigger the soil-water relationship as a non-linear system.

ETHICS STATEMENT

Not applicable.

CONSENT FOR PUBLICATION

Not applicable.

AVAILABILITY OF SUPPORTING DATA

Not applicable.

COMPETING INTERESTS

The author declares that he has no conflict of interest.

FINANCING

We appreciate the support provided by the Secretaría de Ciencia, Humanidades, Tecnología e Innovación SECIHTI, for the postdoctoral stay with number 8085107, as well as to the Earth Sciences Division of FI-UNAM.

AUTHORS' CONTRIBUTIONS

Conceptualization, methodology, formal analysis, preparation of the original draft, writing: review and editing, and acquisition of funding: E.T.S.

ACKNOWLEDGMENTS

We would like to thank the National Autonomous University of Mexico for providing the space to develop this research.

REFERENCES

- Bierawski, L. G., & Maeno, S. (2006). DEM-FEM model of highly saturated soil motion due to seepage force. *Journal of Waterway, Port, Coastal, and Ocean Engineering, 132*(5), 401-409. https://doi.org/10.1061/(ASCE)0733-950X(2006)132:5(401)
- Bronstert, A., Niehoff, D., & Schiffler, G. R. (2023). Modelling infiltration and infiltration excess: The importance of fast and local processes. *Hydrological Processes*, 37(4), 1-20. https://doi.org/10.1002/hyp.14875
- Budhu, M., & Gobin, R. (1996). Slope instability from ground-water seepage. *Journal of Hydraulic Engineering*, 122(7), 415-417. https://doi.org/10.1061/(ASCE)0733-9429(1996)122:7(415)

- Chatra, A. S., Dodagoudar, G. R., & Maji, V. B. (2017). Numerical modelling of rainfall effects on the stability of soil slopes. *International Journal of Geotechnical Engineering*, 13(39), 1-13. https://doi.org/10.1080/19386362.2017.1359912
- Chhorn, C., Hong, S. J., & Lee, S. W. (2014). Critical duration of rainfall-induced landslide. In J. Y. Wu, S.-J. Chao, K. Dai, & S.-R. Yang (Eds.). Innovative and sustainable use of geomaterials and geosystems (Geotechnical Special Publication No. 245. (pp. 161-170). Reston, VA, USA: American Society of Civil Engineers. https://doi.org/10.1061/9780784478455.010
- Collins, B. D., & Znidarcic, D. (2004). Stability analyses of rainfall induced landslides. *Journal of Geotechnical and Geoenvironmental Engineering*, 130(4), 362-372.
- Coras, M. P. M. (1989). Propiedades físicas del suelo relacionadas con el riego. México: Universidad Autónoma de Chapingo.
- Díaz-Puga, M. A., & Mateos, R. M. (2013). Control y seguimiento de una grieta de tracción relacionada con extracciones mineras. Medidas de drenaje. El caso de Padul (Granada) En E. Alonso, J. Corominas, & Hürlimann, M. (Eds.). VIII Simposio Nacional sobre Taludes y Laderas Inestables. (pp. 917-928). Palma de Malorca, España: UPC-CIMNE. ISBN: 978-84-941004-9-9
- Elmaloglou, S., & Diamantopoulos, E. (2008). The effect of intermittent water application by surface point sources on the soil moisture dynamics and on deep percolation under the root zone. *Computers and Electronics in Agriculture, 62*(2), 266-275. https://doi.org/10.1016/j.compag.2008.01.008
- Estabragh, A. R., Soltani, A., & Javadi, A. A. (2016). Models for predicting the seepage velocity and seepage force in a fiber reinforced silty soil. Computers and Geotechnics, 75, 174-181. https://doi.org/10.1016/j.compgeo.2016.02.002
- Feng S., Liu H. W., & Ng, C. W. W. (2019). Analytical solutions for onedimensional water flow in vegetated layered soil. *International Journal of Geomechanics*, 19(2), 04018191. https://doi.org/10.1061/(ASCE)GM.1943-5622.0001343
- Garcia, E., Oka, F., & Kimoto, S. (2011). Numerical analysis of a one-dimensional infiltration problem in unsaturated soil by a seepage-deformation coupled method. International *Journal for Numerical and Analytical Methods in Geomechanics*, 35(5), 544-568. https://doi.org/10.1002/nag.908
- Gascón, B., Bru, G., Camacho, A. G., Avellaneda, M., Prieto, J. F., González, P. J., ... & Fernández, J. (2013). Ladera inestable en Leintz-Gatzaga: Estudio geotécnico y control del deslizamiento con técnicas terrestres y espaciales. En E. Alonso, J. Corominas & M. Hürlimann (Eds.). VIII Simposio Nacional sobre Taludes y Laderas Inestables (pp. 763-774). Palma de Malorca, España: UPC-CIMNE. ISBN 978-84-941407-0-9
- Ghafoori, Y. (2024). Seepage detection using passive temperature measurements by fiber optic DTS. *Informatica, 48,* 285-288. https://doi.org/10.31449/inf.v48i2.5750
- Ghafoori, Y., Maček, M., Vidmar, A., Říha, J., & Kryžanowski, A. (2020). Analysis of seepage in a laboratory scaled model using passive optical fiber distributed temperature sensor. *Water, 12*(2), 367. https://doi.org/10.3390/w12020367
- Griffiths, D. V., & Lu, N. (2005). Unsaturated slope stability analysis with steady infiltration or evaporation using elasto-plastic finite elements. International Journal for Numerical and Analytical Methods in Geomechanics, 29(3), 249-267. https://doi.org/10.1002/nag.413
- Han, Y., Wang, Q., Liu, J., & Li, X. (2022). Seepage characteristics in unsaturated dispersive soil considering soil salinity and density impacts: Experimental and numerical combined study. *Journal of Hydrology*, 614(11), 128538. https://doi.org/10.1016/j.jhydrol.2022.128538
- Hsieh, P. C., & Yang, J. S. (2011). A semi-analytical solution of surface flow and subsurface flow on a slope land under a uniform rainfall excess. International Journal for Numerical and Analytical Methods in Geomechanics, 37(8), 1-11. https://doi.org/10.1002/nag.1128
- Huang, A. B., Lee, J. T., Ho, Y. T., Chiu, Y. F., & Cheng, S. Y. (2012). Stability monitoring of rainfall-induced deep landslides through pore pressure profile measurements. Soils and Foundations, 52(4), 737-747. https://doi.org/10.1016/j.sandf.2012.07.013
- Huang, C. C., & Lo, C. L. (2013). Simulation of subsurface flows associated with rainfall-induced shallow slope failures. *Journal of GeoEngineering*, 8(3), 101-111. https://doi.org/10.6310/jog.2013.8(3).4
- Huang, Z., Bai, Y., & Xu, H. (2022). Impacts of intensive seepage flow on suffusion development in cohesionless soil: Insight from a theoretical model. *Geomechanics for Energy and the Environment, 31*, 1-9. https://doi.org/10.1016/j.gete.2022.100382
- Huang, Z., Bai, Y., Xu, H., Cao, Y., & Hu, X. (2017). A theoretical model to predict the critical hydraulic gradient for soil particle movement under two-dimensional seepage flow. *Water, 9*(11), 1-14. https://doi.org/10.3390/w9110828
- Kosugi, K. I., Uchida, T., & Mizuyama, T. (2004). Numerical calculation of soil pipe flow and its effect on water dynamics in a slope. *Hydrological Processes*, 18(4), 777-789. https://doi.org/10.1002/hyp.1367
- Lazarovitch, N., Ben-Gal, A., Šimůnek, J., & Shani, U. (2007). Uniqueness of soil hydraulic parameters determined by a combined wooding inverse approach. Soil Science Society of America Journal, 71(3), 860-865. https://doi.org/10.2136/sssaj2005.0420
- Li, X., Rendón, L. E., & Espinoza, M. J. (2010). Consideración de fuerzas de filtración en el análisis de estabilidad de taludes granulares. Tecnología y Ciencias del Aqua, 1(3), 89-107.
- Lima, S. N., & Correa-Gomes, L. C. (2018). Study on the gravitational flow directions of the Maracangalha formation (early cretaceous), Bom Despacho, NNE area of Itaparica Island, Bahia, Brazil. *Brazilian Journal of Geology, 48*(3), 503-518. https://doi.org/10.1590/2317-4889201820180061
- López-Acosta, N. P. (2014) Modelado numérico de problemas de flujo de agua. En Memorias de la XXVII Reunión Nacional de Mecánica de Suelos e Ingeniería Geotécnica (pp. 1-14). Puerto Vallarta, Jalisco, México: Sociedad Mexicana de Ingeniería Geotécnica, A.C.
- Lu, N., & Likos, W. J. (2004). Unsaturated soil mechanics. New Jersey, NY, USA: John Wiley & Sons. ISBN: 978-0-471-44731-3
- Lu, N., Kaya, M., & Godt, J. W. (2014). Interrelations among the soil-water retention, hydraulic conductivity, and suction-stress characteristic curves. Journal of Geotechnical and Geoenvironmental Engineering, 140(5), 04014007. https://doi.org/10.1061/(ASCE)GT.1943-5606.0001085
- Luo, Y., Zhang, J. M., Zhou, Z., Shen, Z. J., Chong, L., & Victor, C. (2021). Investigation and prediction of water infiltration process in cracked soils based on a full-scale model test. *Geoderma*, 400, 115111. https://doi.org/10.1016/j.geoderma.2021.115111
- Miyazaki, T. (1988). Water flow in unsaturated soil in layered slopes. *Journal of Hydrology, 102,* 201-214. https://doi.org/10.1016/0022-1694(88)90098-4
- Miyazaki, T. (2006). Water flow in soils. Boca Ratón, FL, USA: CRC Press. https://doi.org/10.1201/9781420030136
- Montgomery, D. R., Schmidt, K. M., Dietrich, W. E., & McKean, J. (2009). Instrumental record of debris flow initiation during natural rainfall: Implications for modeling slope stability. *Journal of Geophysical Research, 114*, 1-16. https://doi.org/10.1029/2008JF001078
- Neris, J., Jiménez, C., Fuentes, J., Morillas, G., & Tejedor, M. (2012). Vegetation and land-use effects on soil properties and water infiltration of Andisols in Tenerife (Canary Islands, Spain). Catena, 98, 55-62. https://doi.org/10.1016/j.catena.2012.06.006
- Pan, Q., Xu, J., & Dias, D. (2017). Three-dimensional stability of a slope subjected to seepage forces. *International Journal of Geomechanics*, 17(8), 04017035. https://doi.org/10.1061/(ASCE)GM.1943-5622.0000913
- Priest, G. R., Schulz, W. H., Ellis, W. L., Allan, J. A., Niem, A. R., & Niem, W. A. (2011). Landslide stability: role of rainfall-induced, laterally propagating,

- pore-pressure waves. Environmental & Engineering Geoscience, 17(4), 315-335. https://doi.org/10.2113/gseegeosci.17.4.315
- Radcliffe, D. E., & Rasmussen, T. C. (2002). Soil water movement En: A. W. Warrick (Ed). Soil Physics Companion (pp. 85-126). Boca Raton, FL, USA: CRC Press. https://doi.org/10.1201/9781420041651
- Rausch, R. (2009). Groundwater modelling an introduction to groundwater flow and solute transporte modeling with applications. Germany: Technische Universitat Darmstadt.
- Rozhko, A.Y. (2010). Role of seepage force on seismicity triggering. *Journal of Geophysical Research*, 115, 1-12. https://doi.org/10.1029/2009JB007182 Sanvitale, N., Zhao, B. D., Bowman, E. T., & O'Sullivan, C. (2023). Particle-scale observation of seepage flow in granular soils using PIV and CFD. *Géotechnique*, 73(1), 71-88. https://doi.org/10.1680/jgeot.20.P.432
- Shin, Y. J., Song, K. I., Lee, I. M., & Cho, G. C. (2011). Interaction between tunnel supports and ground convergence Consideration of seepage forces. *International Journal of Rock Mechanics and Mining Sciences*, 48(3), 394-405. https://doi.org/10.1016/j.ijrmms.2011.01.003
- Teófilo-Salvador, E., Morales-Reyes, G. P., Esteller-Alberich, M. V., & Muciño-Castañeda, R. (2019a). Parámetros que controlan la percolación profunda en un cultivo de trigo. *Terra Latinoamericana*, 37, 57-68. https://doi.org/10.28940/terra.v37i1.345
- Teófilo-Salvador, E., Morales, R. G. P., Muciño, C. R., & Esteller, A. M. V. (2019b). Experimentación reducida-controlada in situ del deslizamiento de suelo por efecto de flujo subsuperficial de agua. *Ingeniería Investigación y Tecnología, 20*(3),1-12. https://doi.org/10.22201/fi.25940732e.2019.20n3.026
- Teófilo-Salvador E., Morales, R. G. P., Muciño, C. R., & Esteller, A. M. V. (2019c). Modelo hidrogeomecánico: masa de suelo+ flujo de agua. Conciencia Tecnológica, 57, 40-45.
- Teófilo-Salvador, E., & Morales-Reyes, G. P. (2018). Propuesta del modelo físico del infiltrómetro de cilindros concéntricos rediseñado multifuncional (ICCRM). *Tecnología y Ciencias del Agua, 9*(6), 103-131. https://doi.org/10.24850/j-tyca-2018-06-05
- Tomlinson, S. S., & Vaid, Y. P. (2000). Seepage forces and confining pressure effects on piping erosion. *Canadian Geotechnical Journal*, 37(1), 1-13. https://doi.org/10.1139/t99-116
- Tosaka, H., Itoh, K., & Furuno, T. (2000). Fully coupled formulation of surface flow with 2-phase subsurface flow for hydrological simulation. Hydrological Processes, 14(3), 449-464. https://doi.org/10.1002/(SICI)1099-1085(20000228)14:3<449::AID-HYP948>3.0.CO;2-9
- Udawatta, R. P., Gantzer, C. J., Anderson, S. H., & Assouline, S. (2016). Synchrotron microtomographic quantification of geometrical soil pore characteristics affected by compaction. Soil, 2(2), 211-220. https://doi.org/10.5194/soil-2-211-2016
- USDA (United States Department of Agriculture) (2004). Soil survey laboratory methods manual. Washington, D.C., USA: United States Department of Agriculture
- Van Asch, T. W., Van Dijck, S. J. E., & Hendriks, M. R. (2001). The role of overland flow and subsurface flow on the spatial distribution of soil moisture in the topsoil. *Hydrological Processes*, 15(12), 2325-2340. https://doi.org/10.1002/hyp.263
- Walpole, R. E., Myers, R. H., Myers, S. L., & Ye, K. (2012). Probabilidad y estadística para ingeniería y ciencias. México: Pearson Educación. ISBN: 978-607-32-1417-9
- Xiang, T., Vivoni, E. R., & Gochis, D. J. (2018). Influence of initial soil moisture and vegetation conditions on monsoon precipitation events in northwest México. *Atmósfera, 31*(1), 25-45. https://doi.org/10.20937/atm.2018.31.01.03
- Xiao, Q., & Wang, J. P. (2020). CFD-DEM simulations of seepage-induced erosion. Water, 12(3), 678. https://doi.org/10.3390/w12030678
- Zhong-ming, H., Hao-long, T., & Xi, D. (2018). Effect of seepage force on stability of high embankment with coarse-grained soil during rainfall. Journal of Highway and Transportation Research and Development, 12(1), 44-52. https://doi.org/10.1061/JHTRCQ.0000609
- Zulkarnain, Z., Kurniawati, R., Triwulandari, T., Husein, I. R., & Kurniawan, R. (2023). Water seepage rate in composted soil. Science, Technology, and Communication Journal, 3(3), 95-100. https://doi.org/10.59190/stc.v3i3.236